A Local Forecast of Land Surface Wetness Conditions Derived from Seasonal Climate Predictions

JEFFREY SHAMAN

Lamont-Doherty Earth Observatory, and Department of Earth and Environmental Sciences, Columbia University, Palisades, New York

MARC STIEGLITZ

Lamont-Doherty Earth Observatory, Columbia University, Palisades, New York

STEPHEN ZEBIAK

International Research Institute for Climate Prediction, Palisades, New York

MARK CANE

Lamont-Doherty Earth Observatory, and Department of Earth and Environmental Sciences, Columbia University, Palisades, New York

(Manuscript received 17 October 2002, in final form 30 January 2003)

ABSTRACT

An ensemble local hydrologic forecast derived from the seasonal forecasts of the International Research Institute for Climate Prediction (IRI) is presented. Three-month seasonal forecasts were used to resample historical meteorological conditions and generate ensemble forcing datasets for a TOPMODEL-based hydrology model. Eleven retrospective forecasts were run at Florida and New York sites. Forecast skill was assessed for mean area modeled water table depth (WTD) and compared with WTD simulated with observed data. Hydrology model forecast skill was evident at the Florida site. Persistence of initial hydrologic conditions and local skill of the IRI seasonal forecast contributed to this local hydrologic forecast skill. At the New York site, there was no persistence of initial hydrologic conditions and local skill of the IRI seasonal forecast was poor; these factors precluded local hydrologic forecast skill at this site.

1. Introduction

Recently, we identified a strong association between mean area water table depth (WTD), as modeled by a dynamic hydrology model (Stieglitz et al. 1997), which we here refer to as the Topographically Based Hydrologic (TBH) model, and transmission of the Saint Louis encephalitis (SLE) virus in Indian River County, Florida (Shaman et al. 2002a). Low modeled WTDs (droughts) during the spring season were shown to restrict vector mosquito activity to select habitats preferred by nesting wild birds. The increased contact of avian hosts and vector mosquitoes facilitated rapid epizootic amplification of the SLE virus. Amplification is a critical component of the SLE transmission cycle (McLean and Bowen 1980), during which the virus is passed between mosquitoes and susceptible hosts, increasing the infection rates in both populations. High mosquito infection rates are necessary for epidemic transmission of the SLE virus to humans.

A strong empirical relationship was found between SLE virus transmission and low modeled WTDs 4 months prior to transmission and a rising of water table 1–2 weeks prior to transmission (Shaman et al. 2002a). The rising modeled WTD, that is, a wetting of the land surface, increases the availability of suitable habitats for the infected mosquitoes and permits their dispersal throughout the county. Consequently, contact between infected mosquitoes and humans increases, and SLE transmission to humans occurs.

It is this finding that motivates the current study: the development of a seasonal forecast of modeled WTD in south-central Florida in order to predict seasonal SLE virus transmission. We here present a method for making ensemble seasonal forecasts of WTD, as modeled by the TBH model.

Seasonal streamflow forecasts have been in use for many years. The National Weather Service (NWS) has used multiple linear regression models to predict seasonal snowmelt runoff volume. Bayesian Markov mod-

Corresponding author address: Dr. Jeffrey Shaman, Lamont-Doherty Earth Observatory, 61 Route 9W, Palisades, NY 10964-8000. E-mail: jshaman@ldeo.columbia.edu

els have also been developed to predict flood events (Krzysztofowicz 1983) and to estimate uncertainties in the NWS streamflow forecasts (Krzysztofowicz and Watada 1986).

Associations between seasonal stream discharge and large-scale, regional climate phenomena, such as the El Niño-Southern–Oscillation (ENSO), have also been documented (Richey et al. 1989; Simpson et al. 1993; Chiew et al. 1998; Schmidt et al. 2001). These associations have been combined with regression or autoregression (Markov) models to create further constrained seasonal streamflow forecasts (Hastenrath 1990; Young and Gall 1992; Piechota et al. 1998; Liu et al. 1998; Berri and Flamenco 1999).

Over the last few decades the NWS has issued Ensemble Streamflow Prediction (ESP) forecasts (Day 1985; Smith et al. 1992; Schaake and Larson 1998). These 3-month, seasonal forecasts of river flow have been developed for many of the river systems throughout the United States. Current conditions, including soil moisture levels and basin snowpack, are used to initialize a physically based rainfall-runoff hydrology model. Local historical records of temperature and precipitation for the location and season are then used to force the hydrology model. Each forcing thus produces a runoff hydrograph based on current conditions and a historical weather pattern. Together these hydrographs comprise an ensemble of runoff scenarios, which in aggregate provide a probabilistic picture of possible future streamflow conditions.

Hamlet and Lettenmaier (1999) adapted the ESP forecast method to include the effects of ENSO and the Pacific decadal oscillation (PDO) at the Columbia River. The authors used these climate phenomena to condition the probabilities of each historical weather pattern. Thus, rather than weight each historical record equally, the forecast state of ENSO and the current state of the PDO were considered, and some historical weather patterns were favored. The resulting conditioned ensemble forecast had increased lead time and improved forecast specificity for April–September.

Here we develop an ensemble forecast of WTD using the TBH model and seasonal forecasts of temperature and precipitation from the International Research Institute for Climate Prediction (IRI). The IRI seasonal forecasts (Table 1) are derived from global climate models (GCMs). The teleconnective effects of regional climate phenomena, such as ENSO and the PDO, as well as local sea surface temperatures (SSTs), are accounted for in this dynamic framework. These forecasts define conditional probabilities of temperature and precipitation, that is, deviations from climatology, given the current and projected state of the global climate system. We use these conditional probabilities to sample historical meteorological records and drive an ensemble hydrologic forecast using the TBH model.

We apply this methodology at two sites: Vero Beach, Florida, where the association between TBH-modeled

TABLE 1. The 11 retrospective IRI seasonal forecasts run at each site. These runs were performed through 2001 for all seasonal forecasts for which both precipitation and temperature predictions were available, and in which at least one of these two variables deviated from climatology.

	Black Rock Forest, NY						Vero Beach, FL					
	Temperature			Precipitation			Temperature			Precipitation		
Date	Low	Moderate	High	Dry	Moderate	Wet	Low	Moderate	High	Dry	Moderate	Wet
JFM 1998	0.45	0.35	0.2	0.4	0.35	0.25	0.55	0.3	0.15	0.2	0.2	0.6
AMJ 1998	0.33	0.33	0.33	0.25	0.3	0.45	0.33	0.33	0.33	0.25	0.35	0.4
JAS 1998	0.33	0.33	0.33	0.25	0.3	0.45	0.2	0.35	0.45	0.33	0.33	0.33
OND 1998	0.33	0.33	0.33	0.4	0.35	0.25	0.6	0.35	0.05	0.4	0.35	0.25
JFM 1999	0.25	0.3	0.45	0.25	0.4	0.35	0.1	0.3	0.6	0.5	0.35	0.15
AMJ 1999	0.2	0.3	0.5	0.33	0.33	0.33	0.2	0.3	0.5	0.4	0.35	0.25
JAS 1999	0.2	0.35	0.45	0.33	0.33	0.33	0.25	0.35	0.4	0.25	0.35	0.4
JFM 2000	0.2	0.35	0.45	0.2	0.35	0.45	0.2	0.3	0.5	0.5	0.35	0.15
AMJ 2000	0.15	0.35	0.5	0.33	0.33	0.33	0.25	0.3	0.45	0.4	0.35	0.25
JAS 2000	0.2	0.3	0.5	0.33	0.33	0.33	—	—	—	—	—	—
JFM 2001	0.2	0.35	0.45	0.33	0.33	0.33	—	—	—	—	—	—
JAS 2001	—	—	—	—	—	—	0.4	0.35	0.25	0.33	0.33	0.33
OND 2001	—	—	—	—	—	—	0.25	0.3	0.45	0.33	0.33	0.33

WTD and SLE transmission has been established; and at the Black Rock Forest experimental watershed, in Orange County, New York. At both sites, the TBH model has been validated by hydrograph comparison [see Shaman et al. (2002b) and below]. Because our overall goal is to produce an SLE forecast, modeled mean area WTD is our forecast metric. Unlike streamflow, modeled mean area WTD is a variable wholly internal to the validated model. Within this validated model framework, however, modeled WTD is a well-constrained quantity and grossly representative of area-integrated wetness conditions. ''Observed'' mean area WTD, used in the assessment of forecast skill, is in fact not observed but produced by forcing the TBH model with observed weather conditions.

Section 2 provides a description of the TBH model. Section 3 gives site descriptions and validation of the TBH model simulations. Section 4 presents the forecast methodology. Results from the retrospective forecasts and an assessment of forecast skill are given in section 5. Section 6 provides discussion.

2. The TBH model

The TBH model employed for this study has been described by Stieglitz et al. (1997). It combines a soil column model, which simulates the vertical movement of water and heat within the soil and between the soil surface plus vegetation and the atmosphere, with the TOPMODEL approach (Beven 1986a,b; Beven and Kirkby 1979), which incorporates the statistics of topography to track the horizontal movement of shallow groundwater from the uplands to the lowlands. The TBH model soil column consists of 10 soil layers. The first soil layer is 4 cm deep; lower-layer depths are defined by a geometric progression. Diffusion and a modified tipping-bucket model govern heat and water flow, respectively (Da Silva and de Jong 1986). The prognostic variables, heat and water content, are updated at each time step. In turn, the fraction of ice and temperature of a layer may be determined from these variables. A three-layer snow model is incorporated in the model structure (Lynch-Stieglitz 1994; Stieglitz et al. 2001). Transpiration and other surface energy balance calculations use a standard vegetation model (Pitman et al. 1991) that includes bare soil evaporation and canopy interception loss. The model has since been updated to account for the effects of shallow subsurface stormflow and variable depth to bedrock (Shaman et al. 2002b).

Consistent with the TOPMODEL approach, the depth of the soil column water table and a probability density function for soil moisture deficit derived from topographic statistics are used to determine the saturated fraction within the watershed (partial contributing area) and groundwater flow discharge. Soil moisture deficit is of the form $\ln(a/\tan\beta)$, where $\tan\beta$ is the local slope angle at a patch on the land surface, and a is the amount of upslope area draining through that patch. This use of TOPMODEL formulations permits the partitioning of runoff and surface water and the energy fluxes without the need to model the landscape explicitly. The combined model produces a three-dimensional picture of soil moisture distribution within a catchment. This approach to modeling the land surface has been validated at several watersheds, ranging in scale from 1.35 km^2 (Shaman et al. 2002b) to 570 000 km^2 (Ducharne et al. 2000).

The TBH model simulates soil column wetness conditions down to depths on the order of meters, that is, the shallow subsurface. By tracking the wetness state of the shallow subsurface, and by accounting for topographic variability, basin river discharge may be well simulated in a TOPMODEL framework (Beven and Kirkby 1979; Sivapalan et al. 1987; Ambroise et al. 1996; Stieglitz et al. 1997). In this framework, the matching of modeled streamflow with measured records implies that mean basin near-surface wetness conditions controlling model streamflow discharge are well constrained. This is particularly true for smaller hillslope catchments in which discharge from deep aquifer waters is minimal. For the sites modeled in this study, deep aquifer discharge contributions to runoff are negligible. In the TBH model, modeled WTD is the variable that best represents the overall wetness conditions of simulated basins.

The TBH model was designed to be forced with an hourly record of seven surface meteorological variables: air temperature, precipitation, relative humidity, surface pressure, wind speed, downwelling longwave radiation, and solar radiation. However, such hourly meteorological data is not available at many locations. For this study, rather than restructure the model to operate with daily forcing of fewer variables (e.g., only temperature and precipitation), we instead use a resampling procedure to generate hourly meteorological records. This process makes use of available hourly datasets in the vicinity of the forecast area and the National Climate Data Center (NCDC) Solar and Meteorological Surface Observation Network (SAMSON) dataset, which provides 30 yr of hourly surface meteorological observations at 262 stations throughout the continental United States. A complete description of the resampling procedure is provided in appendix A.

3. Site descriptions

Two sites were used in this study: the Black Rock Forest experimental watershed in Orange County, New York; and Vero Beach, Indian River County, Florida. The Black Rock Forest experimental watershed was chosen for this study because the hydrology of the catchment is documented and has been well simulated (Shaman et al. 2002b). However, the area is not one in which the IRI seasonal forecast has demonstrated skill—that is, it is a better forecast than climatology (Rajagopalan et al. 2002). The second site, Vero Beach, was chosen

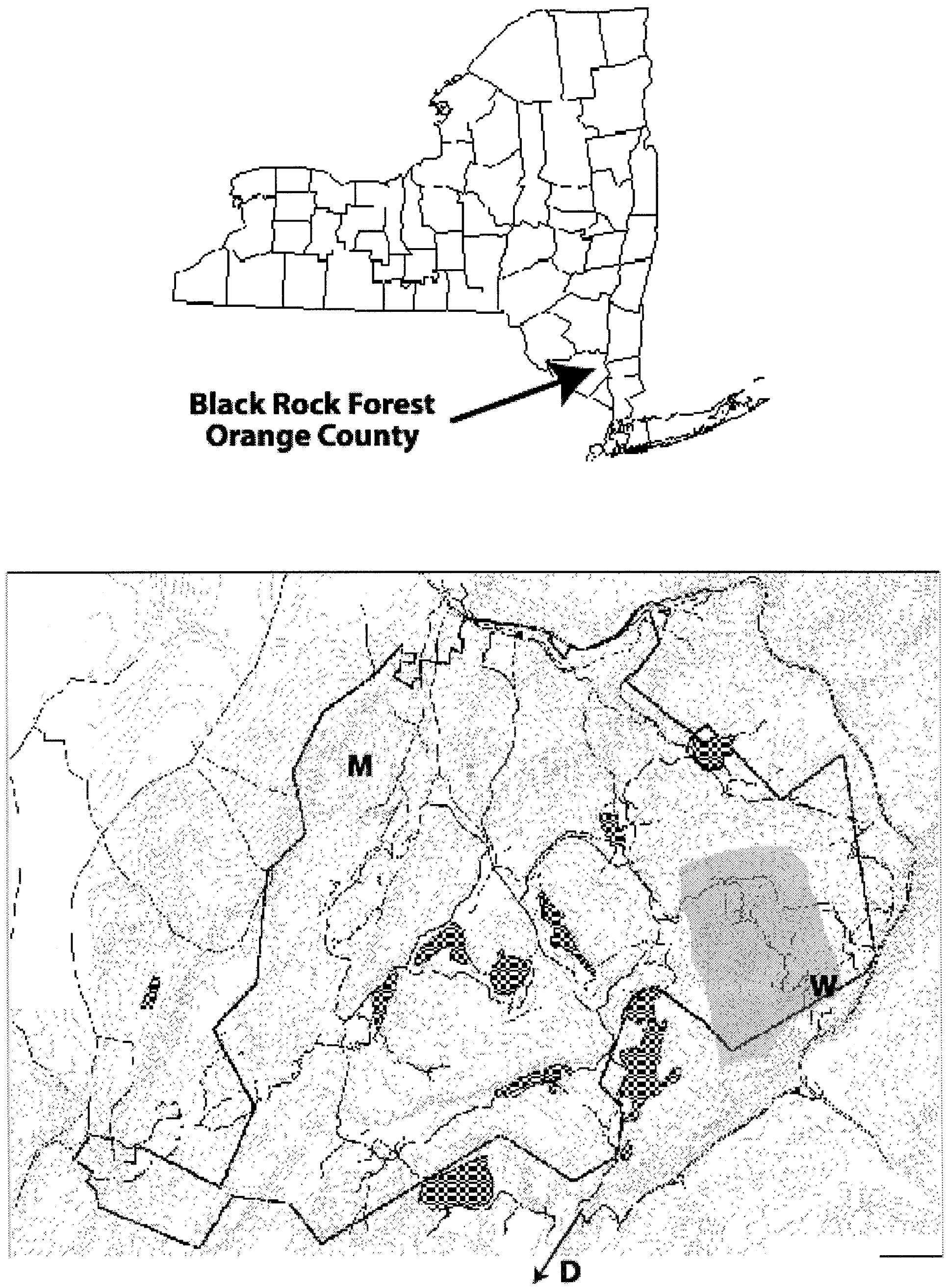

FIG. 1. Map of Black Rock Forest, NY, and the greater area. The catchment simulated (Cascade Brook) is shaded. The location of the weir (W), hourly Black Rock (M), and daily West Point (D) meteorological stations are denoted.

for this study because it is the area in which the incidence of SLE virus transmission has been associated with mean area WTD as represented by the TBH model (Shaman et al. 2002a). It is also an area of good forecast skill (Rajagopalan et al. 2002), due to its proximity to ocean waters, sensitivity to SSTs (Barnett and Preisendorfer 1987), and strong ENSO teleconnection (Ropelewski and Halpert 1986, 1989; Green et al. 1997).

a. The Black Rock Forest experimental watershed

The Black Rock Forest is a 15-km^2 preserve located in the Hudson Highlands region of New York (Fig. 1; Table 2). Within the forest lies Glycerine Hollow, a 1.35-km^2 experimental catchment drained by a single stream, Cascade Brook. Average hourly discharge from Cascade Brook is monitored continuously using a V-notch weir

TABLE 2. Summary of properties at the Black Rock and Vero Beach study sites.

	Black Rock	Vero Beach
Catchment size	1.35 km^2	Unknown
Topography	Steep	Very flat
Vegetation	Deciduous forest	Citrus groves; hammocks
Water control	No	Yes
Snowfall	Yes	No (generally)

installed in 1998. Hourly measurements of precipitation, air temperature, dewpoint temperature, incoming shortwave radiation, and wind speed, taken within the forest, are also available from 1998 to the present. Hourly thermal radiation for the site is calculated following the methodology of Anderson and Baker (1967). Daily records of temperature and precipitation from 1950 to the present are available from the U.S. Military Academy at West Point meteorological station, which is approximately 4 km from the catchment.

For the purposes of resampling, the local hourly meteorological record at Black Rock (1998–01) was supplemented with 1965–90 hourly data from the Wilkes–Barre/Scranton site of the NCDC SAMSON dataset. Seasonal means and ranges of temperature and precipitation, as well as latitude and altitude, are similar to those at Black Rock. A resampled hourly record from 1950 through March 2001 was generated using the West Point daily data, the Black Rock hourly data, and the Wilkes–Barre/Scranton hourly data. The topographic statistics (i.e., probability density function of soil moisture deficit) for the Black Rock watershed were calculated from a 10-m-cell U.S. Geological Service (USGS) National Elevation Dataset Digital Elevation Model (DEM) of the area.

The TBH model was calibrated for January 1998 through September 2000. Figure 2 displays the 1999 hydrograph for Black Rock from a model simulation with the resampled hourly record, as well as the measured hydrographic record (only 1 yr is displayed for better clarity). Hydrograph comparison provides an integrated assessment of the TBH model depiction of area hydrologic processes. The model simulations and weir measurements are well matched in this experimental watershed ($r = 0.91$ and rms error is 1.6×10^{-3} m day^{-1} for 1998–2001). For example, the flood due to Hurricane Floyd in September 1999 is well depicted, as is the large storm event in March 1999. Streamflow is accurately constrained, reflecting a good TOPMODEL-based depiction of mean catchment wetness conditions, including WTD and soil moisture content.

Figure 3 shows a 20-yr time series of modeled weekly mean area WTD (representing mean wetness conditions) for 1980–99. The catchment soils in Black Rock are shallow (modeled to a depth of 1 m), and the terrain is steep. The water table responds rapidly to forcing effects, and there appears to be little persistence. However, driest conditions occur in summer and wettest in winter, as seasonal wetting and drying at this latitude are coordinated by snowpack development and ablation, and leaf flush and fall.

b. *Vero Beach, Indian River County, Florida*

Indian River County is located on the east coast of peninsular Florida (Fig. 4). Area topography is flat, and the landscape is laced with canals facilitating water control and drainage. Citrus groves predominate much of the county (see Table 2). An hourly meteorological da-

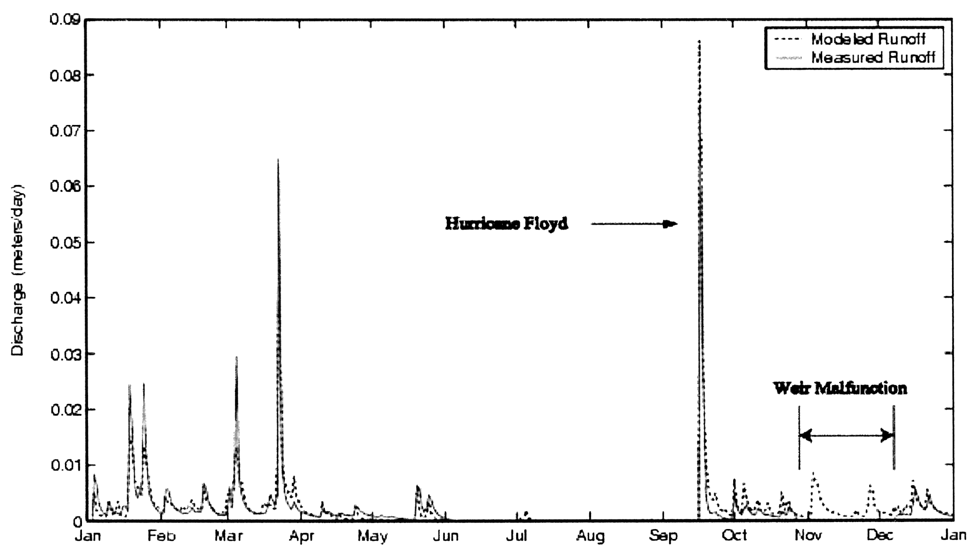

FIG. 2. A 1999 daily streamflow hydrograph for Black Rock from model simulation with the resampled hourly record. The solid line is measured runoff; the dotted line is model simulation of runoff. Streamflow is accurately constrained, reflecting a good depiction of mean catchment wetness conditions within the TOPMODEL framework, including WTD and soil moisture content.

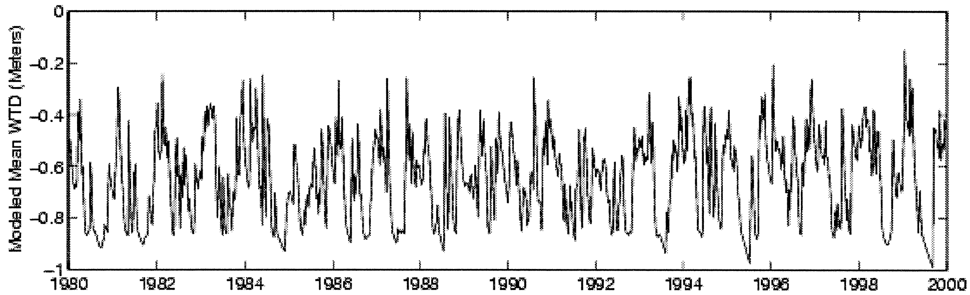

FIG. 3. Time series of weekly mean catchment WTD as modeled at Black Rock, 1980–99. Negative depths (m) indicate distance below the land surface. The water table responds rapidly to forcing effects, and there is little persistence of wetness conditions. Seasonal wetting and drying at this latitude are coordinated by snowpack development and ablation, and leaf flush and fall.

taset from 1984 to 1995 was assembled from NCDC archives for Vero Beach. Solar radiation data were provided by the Northeast Regional Climate Center (NRCC) from analysis of the NCDC data using the NRCC solar energy model (DeGaetano et al. 1995). A 1949–2001 daily record of surface air temperature and precipitation at the Vero Beach 4W meteorological station was downloaded from NCDC archives. This daily record and the 1984–95 hourly record were used to generate a 1949–2001 resampled hourly record.

Topographic statistics for the Vero Beach area were generated from a 10-m-cell USGS DEM of south-central Florida. A 34.9-km^2 catchment, delineated by the TarDEM version 4 freeware routing program (Tarboton 2001), was chosen as a representative watershed and used for model simulations. Discharge data from the USGS South Main Canal in Vero Beach were used for hydrograph validation and model calibration.

Figure 5 shows the measured and modeled hydrographs of mean weekly runoff at the Vero Beach site for 1991. The USGS provides no drainage area for this hydrograph station; normally we would use this area measure to validate the model hydrograph in units of meters per day. This division (removal of the area) would reduce any errors caused by incorrect delineation of the watershed basin boundaries. In Florida, this is particularly problematic due to the flat lay of the land and channelization, which make basin boundary determination suspect. We aligned the model watershed as best we could with the South Main Canal. Hydrograph validation is performed in units of cubic meters per day.

Due to channelization and water control in this south Florida area, measured canal discharge is often altered during storm events and will differ from the TBH model simulation. Channelization increases runoff rates locally, but other effects, including damming, diversion, and tidal flow, can suppress runoff levels. The interaction of these factors produces a noisier, less predictable runoff signal. Still, the model captures storm event timing and the relative magnitudes of runoff volume. Correlation of the daily modeled and measured hydrographs for 1984–95 is $r = 0.34$ ($p < 0.001$); weekly smoothed correlation is $r = 0.61$ ($p < 0.001$); and monthly smoothed correlation is $r = 0.68$ ($p < 0.001$). Fortunately, the longer time periods are most relevant for our purposes.

Model partitioning of runoff and evapotranspiration also match bulk estimates taken from USGS sources (Sumner 2001). In addition, daily fluctuations in the height of groundwater well IR0312, a confined artesian aquifer (see Fig. 4 for location), provided by the St. John's River Water Management District for 1983–2001, are well correlated with modeled mean area WTD ($r = 0.66$). It must be noted that the dynamics of this confined aquifer are not simulated in the TBH model and should not be considered the same quantity as modeled WTD. Recharge of the IR0312 well occurs to the west of Indian River County, and aquifer levels drop during drought when agricultural and homeowner usage of these groundwaters increases. Much of the correlation we found between modeled WTD and the IR0312 well is no doubt due to this human response to drought conditions, not natural fluctuations within the aquifer. However, both modeled WTD and the IR0312 well measurements are indicative of drought conditions, the former through simulation of near-surface wetness conditions, the latter because of the human response to drought conditions (increased use of aquifer waters).

The metric we wish to forecast, modeled mean area WTD, is not a measured quantity. Rather, it represents the aggregate wetness of the near-surface soil column and the extent of surface water pooling. By validating the TBH model with streamflow, bulk partitioning of discharge and evapotranspiration, and groundwater measurements to the extent we have been able at Vero Beach, we assert that modeled mean area WTD is a constrained quantity that simulates area wetness and drought. Krzysztofowicz (1991) has suggested that mean WTD can be used as a variable indicator of drought. Viewed through time, modeled mean area WTD provides a record of the relative wetness in the area, with the highs and lows representing wet and dry conditions, respectively.

We would like to stress that in the Florida environment both the South Main Canal streamflow and the IR0312 groundwater well validation records are subject

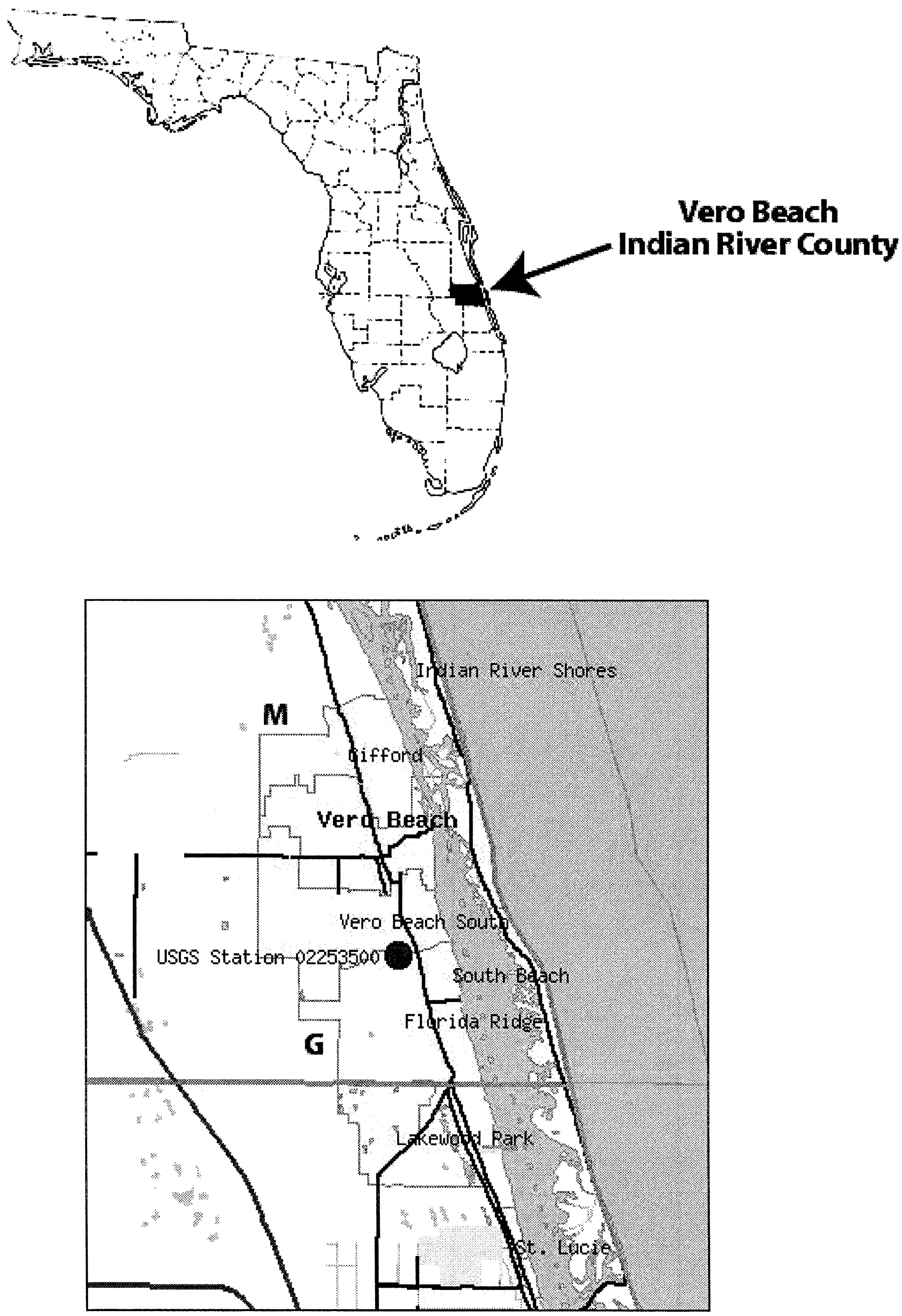

FIG. 4. Map of the Vero Beach, Indian River County, FL, site. The locations of the USGS South Main Canal discharge measurement, groundwater well IR0312 (G), and the Vero Beach 4W meteorological station (M) are indicated.

to numerous confounding factors. It is for these reasons that validation of modeled WTD forecasts is performed internally to the model, not against groundwater well IR0312 measurements. In doing so, we assume that the TBH model correctly simulates the relative wetness of the near-surface soil column in the modeled area.

Figure 6 displays the 1980–99 time series of modeled weekly mean area WTD at Vero Beach. Unlike Black Rock, the Vero Beach site is subject to year-round plant activity, a flatter topography that reduces runoff rates, the absence of snow, and a deeper soil column. The depth of the water table also varies on longer timescales at Vero Beach than at Black Rock, suggesting greater system memory and persistence of wetness condition anomalies. Some years remain very wet; other years remain very dry.

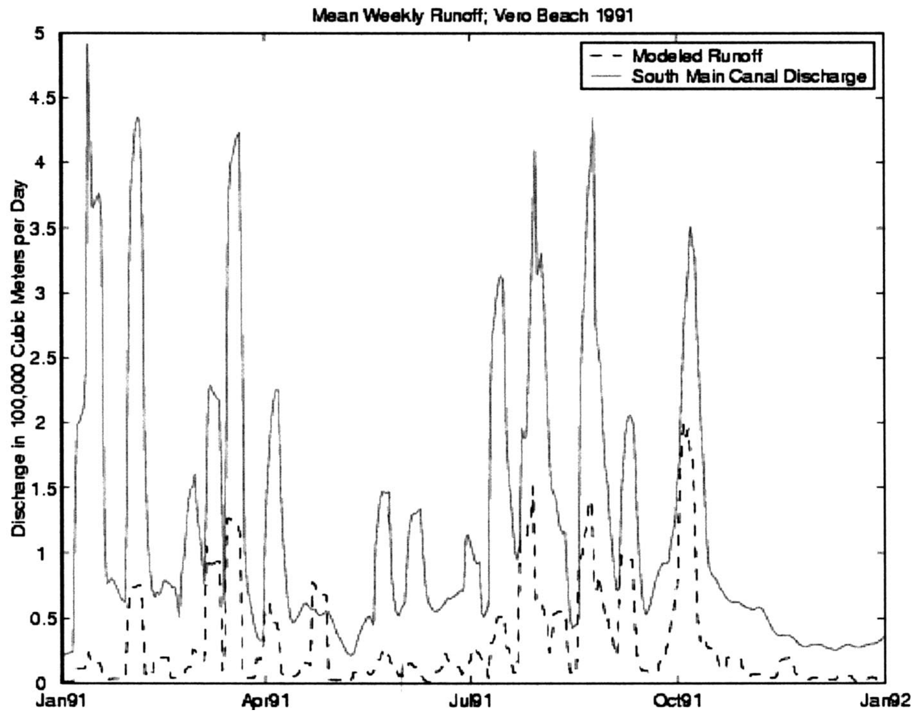

FIG. 5. The 1991 weekly streamflow hydrograph for Vero Beach from model simulation with the resampled hourly record. The solid line is runoff measured at the South Main Canal, Vero Beach; the dotted line is model simulation of runoff. Units are m^3 day^{-1}. Due to channelization, water control, and an uncertain drainage area, the magnitudes of discharge are not well matched; however, the weekly modeled and measured hydrographs are well correlated ($r = 0.61$).

4. Methods

a. Forecast methodology

The IRI seasonal forecasts provide forecast probabilities for precipitation and temperature (Mason et al. 1999). Historical records based on station or regional data are used to delineate tercile boundaries for each variable. The forecast is then issued as the probability of a variable falling within each tercile. Forecasts are provided globally at $2° \times 2°$ resolution; however, forecast skill varies with location (Rajagopalan et al. 2002).

Table 1 provides a listing of the IRI seasonal forecasts used in this study. Runs were performed through 2001 for all seasonal forecasts for which both precipitation and temperature predictions were available, and for which at least one of these two variables deviated from climatology. These seasonal forecast probabilities of precipitation and temperature were used to generate forecast forcing ensembles for the hydrology model. The methodology is as follows. At Black Rock and Vero Beach the resampled hourly records (1950–97 and 1949–97, respectively) are used to determine tercile boundaries for both temperature and precipitation. For instance, July–August–September (JAS) tercile boundaries for precipitation at Black Rock are determined by totaling the 3-month JAS precipitation record of each year of the resampled hourly record, ordering these totals, and using the 33d and 66th percentiles as boundaries to group the records in dry, moderate, and wet bins. The IRI seasonal forecast probabilities are then

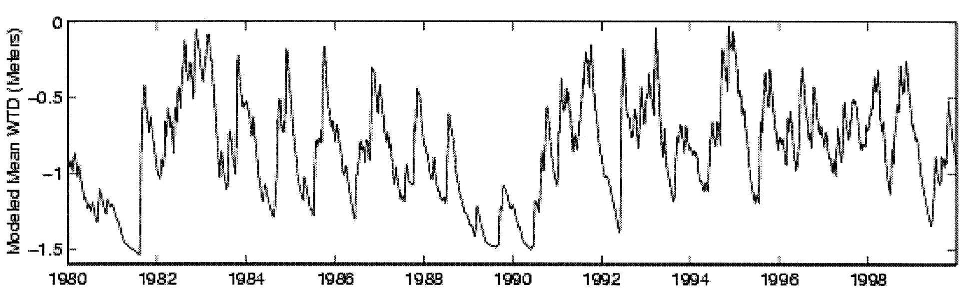

FIG. 6. Time series of modeled weekly mean area WTD as modeled at Vero Beach, 1980–99. Negative depths (m) indicate distance below the land surface.

used to sample randomly within the bins and generate a 500-member forecast forcing ensemble. This binning and random sampling is performed in 3-month blocks, thus preserving the statistical structure of multiday meteorological events. For instance, the forecast over Black Rock for JAS 1998 (see Table 1) predicts a 45% chance of wet tercile conditions; therefore, an ensemble forecast is generated in which 225 of the records are randomly chosen from among the wettest third of local historic hourly JAS meteorological scenarios.

To increase the sample size used to delineate the tercile boundaries, resampled hourly records were used beginning from -10, -5, 0, $+5$, and $+10$ days of the seasonal forecast. Thus, for the JAS example, totals of precipitation were made for each year of the resampled hourly record for the 92 days beginning 21 June, 26 June, 1 July, 6 July, and 11 July. This provided a fivefold increase in meteorological scenarios from which climatology was derived and forcing forecasts were generated. Five- and 10-day shifts were chosen to provide more variability among seasonal records than 1- and 2-day shifts would afford. By staying within ± 10 days, temperature and solar insolation intensities remain representative of local conditions for the time of year.

The IRI seasonal temperature and precipitation forecasts were used jointly to select hourly meteorological scenarios for the ensemble forecasts. At present, these seasonal forecasts are issued as marginal probabilities—that is, they are independent of one another. Thus, for each local hydrological forecast, three potential constraints are available: the marginal seasonal forecast of precipitation; the marginal seasonal forecast of temperature; and the local, seasonal historic joint distribution based on climatology. A variety of weighting schemes are available by which these data can be combined (e.g., preserving one or both marginal probabilities, maintaining ratios within the historic joint distribution, etc.). We tested two such schemes: an independent scheme, in which the historic joint distribution is ignored and only the marginal probabilities are used; and a weighted scheme, in which the marginal probabilities are maintained and some of the local historic (climatological) dependence of precipitation and temperature on one another is preserved. The effect of weighting with the historic joint distribution was small; consequently, little difference in forecast skill was found between the two schemes. For brevity we only present the independent scheme.

The independent scheme forecasts were produced by multiplying the marginal seasonal forecast probabilities of temperature and precipitation. At both sites, 11 such independent joint distribution forecasts were generated, using the IRI seasonal forecasts listed in Table 1. From these joint distribution forecasts, 500-member retrospective forecast ensembles were then generated. In running each ensemble, the TBH model was spun up and forced with the resampled hourly record up to the point of forecast (e.g., for the JAS 1998 forecast, the model was run with the resampled hourly record through 30 June 1998). The final 3 months were then forced with a member of the ensemble. This process was repeated for each member of each 500-member ensemble. A single 3-month simulation was also performed using the observed meteorological record.

TABLE 3. Max, min, and tercile values of WTD from three initial condition ensembles, AMJ 1998, 1999, and 2000, and from the modeled WTD climatology for AMJ. Units are m (below the surface).

	Vero Beach			
	AMJ 1998	AMJ 1999	AMJ 2000	AMJ
Max	−0.280	−0.657	−0.740	−0.653
66%	−0.644	−1.094	−1.187	−0.980
33%	−0.789	−1.199	−1.302	−1.161
Min	−0.881	−1.277	−1.376	−1.485

b. *The climatologies*

For the purposes of comparison and assessment of forecast skill two climatologies were constructed. The first of these, which we refer to as a *modeled WTD climatology,* was derived from single runs of the hydrology model with the full, resampled hourly records at Black Rock and Vero Beach. These runs respectively provided 48 and 49 yr of continuous simulation of modeled WTD. The second type, which we refer to as an *initial condition ensemble,* was constructed in the same fashion as the forecast ensembles, but by assuming a climatological seasonal forecast, that is, a one-third probability seasonal forecast for each tercile of precipitation and temperature.

The modeled WTD climatologies have a fixed distribution for a given season and location. However, the distributions of the initial condition ensembles vary from year to year and are dependent on land surface conditions directly preceding the ensemble run; that is, AMJ 1998 is not same as AMJ 1999. As an example, Table 3 shows the Vero Beach tercile probabilities for AMJ 1998, AMJ 1999, and AMJ 2000 from the initial condition ensembles, as well as for AMJ from the modeled WTD climatology. The three initial condition ensembles do not produce the same distribution of modeled WTDs, even though all three were generated using the same seasonal distribution of weather conditions. These differing tercile probabilities are due to different initial conditions, that is, differing states of water and heat within the model soil column on 31 March 1998, 1999, and 2000. At Vero Beach, the initial conditions used for each initial condition ensemble persist over the 3-month run period and bias the initial condition ensemble distributions. For instance, AMJ 1998 is much wetter than the other years. In distinction, the modeled WTD climatology for AMJ at Vero Beach is built from a distribution of initial 31 March conditions (1949–97), as well as the seasonal distribution weather conditions.

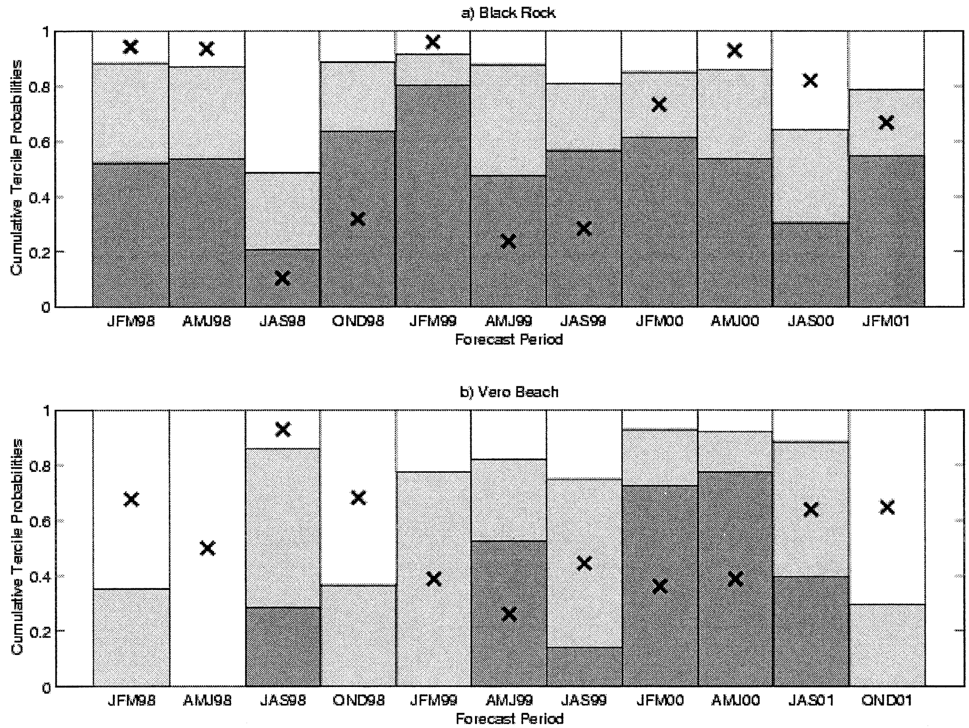

FIG. 7. Bar plots of tercile binning of the forecast ensembles based on boundaries established from the modeled WTD climatology. Probabilities are cumulative. Dark gray indicates the percentage of the ensemble forecast predicted to be in the driest third of climatological conditions. Light gray indicates the percentage of the ensemble forecast predicted to be in the middle third of climatological conditions. White indicates the percentage of the ensemble forecast predicted to be in the wettest third of climatological conditions. The tercile bin in which the simulation with observed meteorological conditions fell is marked by ''X.'' The plots are (a) the 11 retrospective forecasts at Black Rock and (b) the 11 retrospective forecasts at Vero Beach.

(It possesses a broader range of climatological conditions and is, in a stricter sense, the true climatology.)

For this study, we performed three sets of comparisons: 1) comparison of the forecast ensembles with modeled WTD climatology; 2) comparison of the initial condition ensembles with modeled WTD climatology; and 3) comparison of the forecast ensembles with their corresponding initial condition ensembles. The first of these comparisons examines the hydrologic predictive skill gained by both knowledge of initial hydrological conditions and the local seasonal forecast of weather conditions. The second comparison examines the hydrologic predictive skill gained with only knowledge of the initial hydrologic conditions. The third comparison examines the hydrologic predictive skill gained from only the IRI seasonal forecast of weather conditions.

5. Results

a. Forecast modeled water table depth

Figure 7 shows the deviations of forecast ensembles from modeled WTD climatology. Three-month averages of modeled WTD climatology for each season were used to establish tercile boundaries. The 3-month averages of the forecast ensembles were then binned according to these tercile boundaries. Also shown are the bins in which the 3-month average of modeled WTD for simulation with the observed meteorological record fell (indicated by ''x''). From these binnings it is evident that the forecasts at Vero Beach produce a good prediction of future hydrologic conditions. For instance, when the forecast predicts a high probability of dry conditions, that is, greater than the climatological one-third probability, real-data simulated conditions are often dry. At Black Rock, however, the forecasts are often poor, predicting very high probabilities (>0.5) for conditions that are not realized.

Figure 8 shows the deviations of the initial condition ensembles from the modeled WTD climatology. Again, at Vero Beach there appears to be good prediction of future hydrologic conditions, but at Black Rock the predictions are poor. These results suggest that at Vero Beach, knowledge of initial conditions, combined with climatological forcing, is adequate to produce a good forecast.

Figure 9 shows the deviations of the forecast ensembles from their initial condition ensemble counterparts. In this analysis, 3-month averages of modeled WTD for

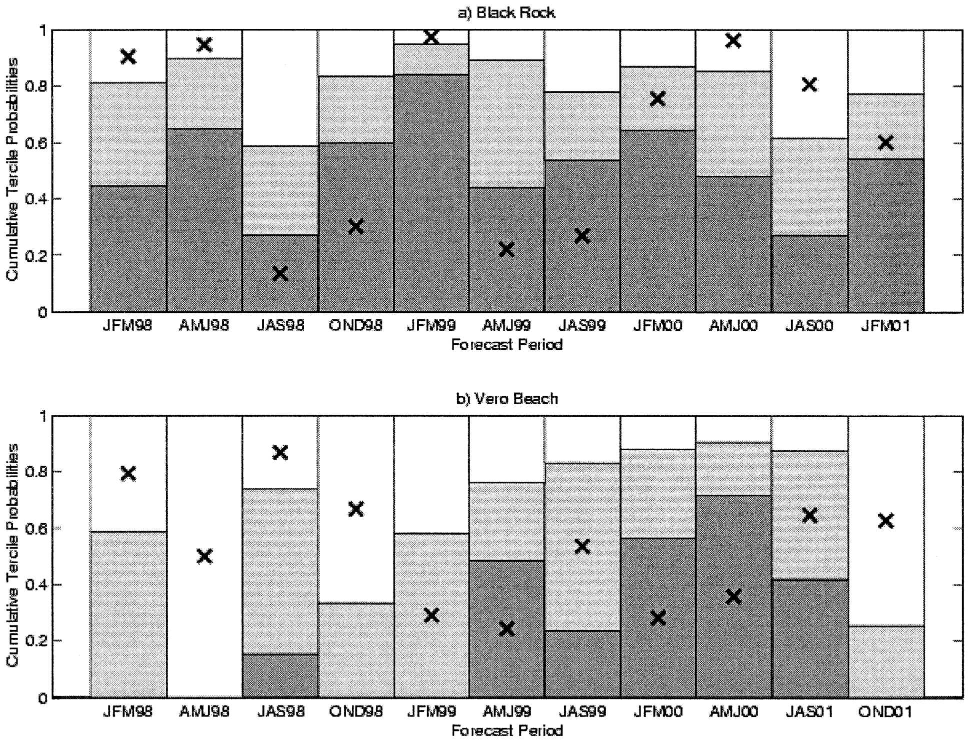

FIG. 8. As in Fig. 7, bar plots of tercile binning of the initial condition ensembles based on boundaries established from the modeled WTD climatology.

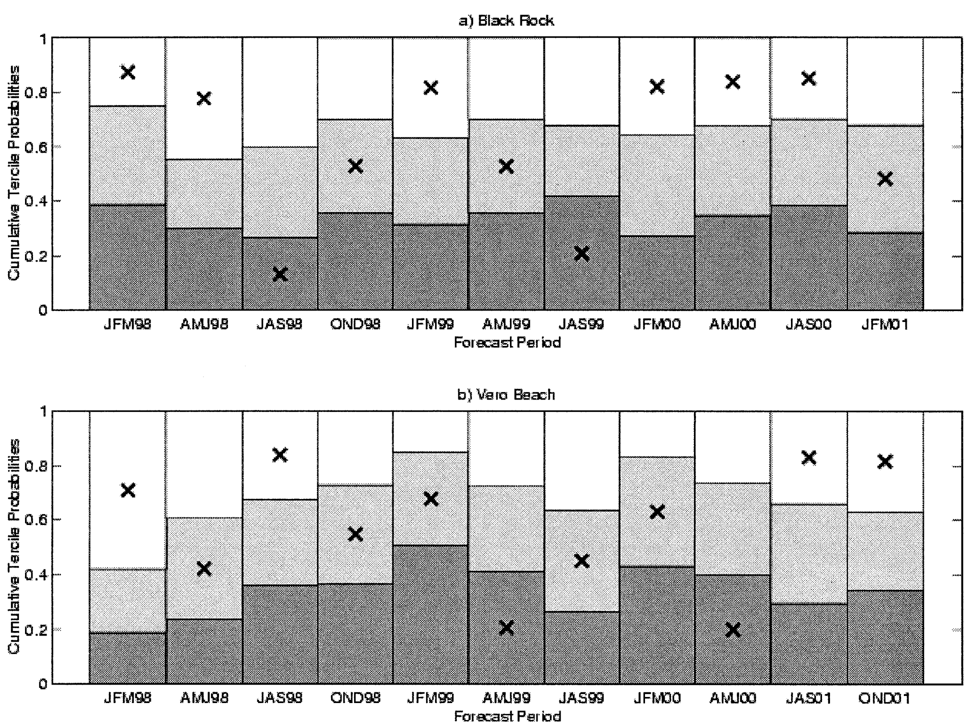

FIG. 9. As in Fig. 7, bar plots of tercile binning of the forecast ensembles based on boundaries established from counterpart initial condition ensembles.

TABLE 4. Ranked probability skill scores and their statistical significance at Black Rock and Vero Beach based on all 11 retrospective ensembles. Three comparisons are presented for each site. RPSS and significance were calculated for tercile binning and are shown for varying time periods of the 3-month forecast. Values significant at $p < 0.05$ are in boldface; * values are significant at $p < 0.001$.

	Forecast ensemble vs modeled WTD climatology		Initial condition ensemble vs model WTD climatology		Forecast ensemble vs initial condition ensemble	
Site	Black Rock	Vero Beach	Black Rock	Vero Beach	Black Rock	Vero Beach
First month	−0.31	**0.89***	−0.25	**0.87***	−0.07	−0.00
Second month	−0.21	**0.57***	−0.20	**0.50***	−0.00	**0.04**
Third month	−0.26	**0.39***	−0.27	**0.28***	−0.03	**0.14***
All 3 months	−0.35	**0.66***	−0.35	**0.54***	0.00	**0.14***

each member of an initial condition ensemble were used to establish tercile boundaries. The 3-month averages of its counterpart forecast ensemble were then binned according to these tercile boundaries. IRI seasonal forecasts of temperature and precipitation with larger deviations from climatology tended to produce greater deviations from climatology for modeled WTD. Also shown are the bins in which the 3-month average of modeled WTD from simulation with the observed meteorological record resides. Based on these binnings, it appears that the hydrologic predictions at Vero Beach are not as good when the effects of initial conditions are excluded; however, the predictions of future hydrologic conditions at Vero Beach still appear to be better than the predictions for Black Rock.

b. *Assessment of forecast skill*

To assess the forecast skill more formally, we used the Ranked Probability Skill Score (RPSS) (Wilks 1995) (see appendix B for details). Three RPSS analyses were performed. In the first analysis we compare the forecast ensembles with modeled WTD climatology. Table 4 shows the RPSS calculated for the 11 forecast ensembles at Black Rock and Vero Beach for monthly and seasonal forecast time periods. At Vero Beach there are significant levels of skill for month-long and longer intervals ($p < 0.001$); however, at Black Rock no forecast skill is evident.

In the second analysis, we compared the initial condition ensemble with modeled WTD climatology. Table 4 also shows the RPSS calculated for the 11 initial condition ensembles at Black Rock and Vero Beach for a range of forecast time periods. Again, at Vero Beach, highly significant levels of skill are evident at month-long and longer intervals ($p < 0.001$), though these RPSS values are not as high as for the forecast ensembles. This result again shows that the simple use of initial hydrologic conditions and climatological weather conditions produces a skillful seasonal forecast of local hydrologic conditions at Vero Beach. It demonstrates the persistence of wetness conditions at this site. At the faster responding Black Rock site, however, no skill of forecast is evident.

For the third analysis, we compared the forecast ensembles with the initial condition ensembles. Table 4 shows the RPSS calculated for the 11 forecast ensembles at Black Rock and Vero Beach for a range of forecast time periods. Again, there is no skill evident at Black Rock; however, at Vero Beach, there are significant levels of skill for forecasts of the second and third months ($p < 0.05$, 0.001) and all 3 months of the season ($p < 0.001$), indicating that a significant level of skill is contributed by the IRI seasonal forecasts.

6. Discussion

We find local hydrologic forecast skill at Vero Beach, Florida, but not at Black Rock Forest, New York. Two factors contribute to the hydrologic forecast skill at Vero Beach: persistence of hydrological anomalies, and skill of the IRI seasonal forecast of temperature and precipitation. The RPSS analyses at Vero Beach show that some skill is added through use of the IRI seasonal forecast distributions, but that most of the forecast skill derives from knowledge of the initial wetness state at the time of forecast.

Comparison of the initial condition ensembles and modeled WTD climatology demonstrates the sensitivity of the land surface to initial wetness conditions and provides evidence for the seasonal persistence of WTD anomalies at Vero Beach. Use of climatological forcing conditions in conjunction with known initial wetness conditions produces a skillful local hydrologic forecast. Such an ensemble forecast is very similar to the NWS ESP forecasts. Thus, in the absence of a seasonal forecast of temperature and precipitation, a skillful local seasonal forecast of modeled WTD could still be produced at Vero Beach.

Figure 10 shows lag autocorrelation diagrams of modeled mean area WTD at both the Black Rock and Vero Beach sites. The Vero Beach site possesses a much longer decorrelation length than Black Rock; at 90 days, the lag autocorrelation at Vero Beach is still $r = 0.45$, whereas at Black Rock it is $r = -0.02$. These differences provide evidence for the seasonal persistence of wetness anomalies at Vero Beach but not at Black Rock.

Examination of Figs. 3 and 6 provides further evi-

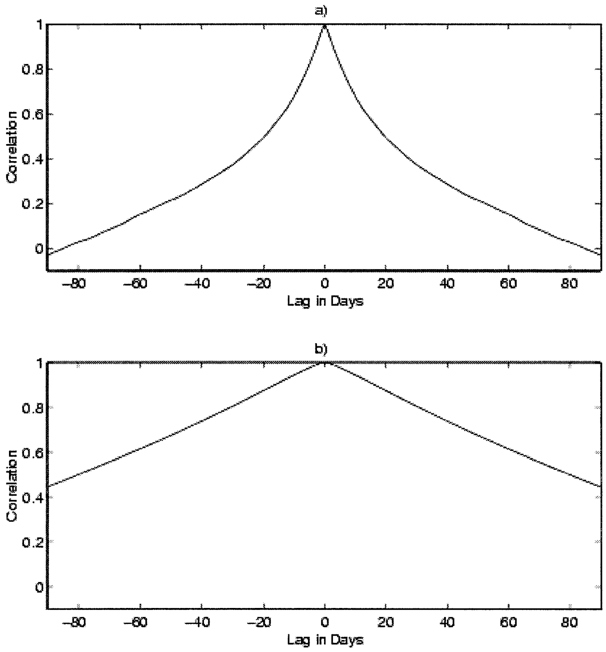

FIG. 10. Lag autocorrelation diagrams of daily mean area WTD as model simulated at (a) Black Rock, 1950–2001 and (b) Vero Beach, 1949–2001.

dence for the seasonal persistence of WTD anomalies at Vero Beach but not at Black Rock. The Florida site is much more slowly varying and possesses a more pronounced interannual variability than the New York site. At Vero Beach, model system water loss occurs predominantly through evapotranspiration, which accounts for over 80% of the total precipitation. At the steeper-sloped and shallower-soiled Black Rock site, runoff and evapotranspiration contribute equally to water loss (data not shown). Consequently, anomalies persist longer at Vero Beach, whereas Black Rock dries more quickly. Furthermore, other factors controlling land surface hydrology, such as snowpack development and ablation, and leaf flush and fall, occur at the temperate New York site. These processes define a more regular seasonal cycle at Black Rock and return local wetness conditions to a preferred seasonal mean state. At Vero Beach, where these processes are not present, pronounced anomalies may persist through several seasons.

Because land surface hydrology is more simply controlled in Florida, that is, water comes into the system via precipitation and leaves predominantly through year-round evapotranspiration, the area is more sensitive to weather anomalies. The comparison of the forecast ensembles with the initial condition ensembles demonstrates this sensitivity. At Vero Beach, the skill of the IRI seasonal forecast downscales through to the local, seasonal (3 month) hydrologic forecast. Most of this ''downscaled'' skill is derived from the precipitation forecast. Comparison of Table 1 and Fig. 9 reveals that the seasonal forecast probabilities for precipitation closely matched the outcome binning (wet, moderate, dry) of modeled WTD when the effects of initial conditions are accounted for. On the other hand, at Black Rock, the IRI seasonal forecast has poor skill (Rajagopalan et al. 2002), and the hydrology of the area is significantly affected by runoff, snowpack processes, and seasonal plant activity. Consequently, no local hydrology forecast skill is gained through downscaling of the IRI seasonal forecast at Black Rock.

The method described here could be adapted for use with other hydrology models, including statistical (regression) models. A means of accounting for current wetness conditions would be needed; then an ensemble of trace forecasts would need to be run through the regression model using conditional probabilities based on the IRI seasonal forecasts. We do not believe that either dynamic or statistical models are intrinsically superior; rather, each form has its advantages. Much as a number of statistical and dynamic models are used for ENSO forecasting (Barnston et al. 1999), a suite of model types used for hydrologic forecasting would likely provide more skillful predictions.

The TBH model used in this study was designed to be run as the land surface component of a GCM, and as such was structured as a physically based hydrology model driven by hourly input. When run offline, as in this study, we maintain the hourly time step structure that has been validated and applied to numerous watersheds (Stieglitz et al. 1997; Ducharne et al. 2000; Stieglitz et al. 2000; Shaman et al. 2002b). We expect that a daily time step hydrology model, used with the methodology presented in this study, would produce similarly skillful seasonal hydrologic forecasts. Historical daily data are more readily available than hourly; however, generation of the resampled hourly record is not particularly time consuming. Hourly datasets needed for resampling, such as the NCDC SAMSON dataset, are readily available. In addition, the Global Energy and Water Cycle Experiment (GEWEX) Continental-Scale International Project (GCIP) Land Data Assimilation System (LDAS) Project has begun producing a real-time, hourly, distributed simulation of land surface conditions at 0.125° resolution for the entire continental United States (Mitchell et al. 1999).

Our results suggest that skillful local hydrologic forecasts using the described methodology should be possible in regions where WTD anomalies tend to persist. Such areas will have a less responsive water table and may have fewer processes controlling the local hydrologic cycle. Tropical and subtropical regions, as well as flatter areas, often meet these criteria and may yield skillful hydrologic forecasts. Areas where the IRI seasonal forecast has demonstrated skill would also be candidates for this type of local hydrologic forecast.

Use of the methodology presented will enable operational forecasts of local near-surface wetness conditions in areas of seasonal forecast skill, and permit application of these hydrological forecasts to water management, public health, and agricultural decision making. As understanding of regional climate phenomena and the global climate system improves, so should seasonal forecasts of precipitation and temperature. These improvements should in turn lead to improvements of hydrologic forecast skill.

The hydrological forecast at Vero Beach is representative of an operational application, in which hydrological conditions are modeled outside the bounds of an experimental watershed, and where human activity—urbanization and water control—have altered the natural environment. While such activity limits the accuracy of hydrologic simulation, provided that hydrology model behavior is appropriately constrained and the seasonal forecasts have demonstrated skill, predictions within the limits of accuracy of the hydrology model may still be realized. At Vero Beach, where IRI seasonal forecast skill is good, forecasts of mean area WTD, dependent on antecedent conditions, vegetation and soil types, topography, and seasonal forecast probabilities, appear to be authenticated by comparison to the model forced with observed meteorological conditions. These forecasts will permit probabilistic prediction of future hydrologic conditions. In the Vero Beach area, we have demonstrated the link between modeled WTD and amplification and transmission of the Saint Louis encephalitis virus (Shaman et al. 2002a). We are currently producing a seasonal forecast of these disease-related variables.

Acknowledgments. J. Shaman is supported by a NASA Earth System Science Fellowship. This research was supported by NOAA Grant Number UCS10PO10216264, the NASA Seasonal-to-Interannual Prediction Project at Goddard Space Flight Center, and NASA's Global Modeling and Analysis Program under RTOP 622-24-47. We thank K. Warrach for compiling the West Point daily data, and B. Rajagopalan, J. Day, A. Kaplan, A. Karspeck, and M. Kelley for helpful discussions.

APPENDIX A

Generation of the Resampled Hourly Forcing Meteorological Records

Local hydrologic forecast with the TBH model requires a lengthy hourly record of the seven forcing meteorological variables. This hourly record is needed for both determination of local climatological weather conditions and generation of ensemble forecasts. However, for most areas, hourly records of these seven forcing variables are limited or discontinuous. Rather than supplement such patchy records with hourly records derived from other locales, which may introduce unwanted biases, we instead use local daily surface records of precipitation and temperature to resample the more limited, local hourly record, generating a single, lengthy, continuous record.

The resampling is performed as follows. Each daily record of precipitation and temperature is compared, using a least squares fit, to all years of the same day of hourly records, plus or minus 10 days. For instance, a daily record from 11 January would be compared with hourly records from all available years for the dates 1–21 January. For each of the hourly records, total precipitation and mean temperature are determined. All seven variables of the day-long hourly record with total precipitation and mean temperature most closely matched by least squares fit to the daily record are then selected. The hourly precipitation and temperature are then scaled to match the daily totals exactly, and the mixing ratio is corrected to prevent supersaturation. This resampling procedure is used both to extend the local hourly record and to fill in large gaps. We refer to these extended datasets as resampled hourly records.

Resampling available hourly records in the forecast area creates hourly conditions with variability consistent with local climatology. But clearly different hourly sequences can have the same daily mean temperature and total precipitation. We stress, however, that in the course of this study, no attempt is made to analyze forecast skill on hourly, or even daily, timescales. The timescales of forecast are months and seasons. We merely generate the hourly data to accommodate the TBH model interface. (The TBH model was designed to run as the land surface component of a GCM. Such models require short time steps, i.e., hourly or shorter.)

To test whether biases were introduced by the resampling procedure, time periods for which local hourly data were available were also resampled, but with choice of the correct hourly record precluded (thus the resampled hourly record had to differ from the original). The original hourly record and the resampled hourly record were then used to force the TBH model, and the results compared. Biases were nominal, and the simulations of WTD were highly correlated.

APPENDIX B

Ranked Probability Skill Score (RPSS)

The RPSS is computed by obtaining a ranked probability score (RPS) of WTD for each ensemble (Wilks 1995). We use a climatology (either the initial condition ensembles or modeled WTD climatology) to establish percentile boundaries, then bin the corresponding forecast ensemble using those boundaries. The forecast RPS is then calculated as follows:

$$\mathrm{fRPS}_{kt} = \sum_{m=1}^{J} (F_{mt} - O_{mt})^2, \tag{B1}$$

where fRPS_{kt} is the forecast ranked probability score at location k (Black Rock or Vero Beach) for seasonal forecast t, F_{mt} is the cumulative probability of the forecast ensemble for bin m and seasonal forecast t, O_{mt} is the cumulative probability of the observation (in this case, WTD simulation with the observed meteorological record) for bin m and seasonal forecast t, and J is the number of bins. Since there is only one realization of actual meteorological events, the observed cumulative probabilities equal either 0 or 1.

Similarly the climatological RPS score is obtained by computing

$$\mathrm{cRPS}_{kt} = \sum_{m=1}^{J} (C_{mt} - O_{mt})^2, \qquad \text{(B2)}$$

where cRPS_{kt} is the climatological ranked probability score at location k for seasonal forecast t, C_{mt} is the cumulative probability of the climatology for bin m and seasonal forecast t, O_{mt} is the cumulative probability of the observation for bin m and seasonal forecast t, and J is the number of bins. (For tercile binning, $C_{1t} = 1/3$, $C_{2t} = 2/3$, and $C_{3t} = 1$.)

The RPSS at location k is then computed as

$$\mathrm{RPSS}_k = 1 - \frac{\frac{1}{n}\sum_{t=1}^{n} \mathrm{fRPS}_{kt}}{\frac{1}{n}\sum_{t=1}^{n} \mathrm{cRPS}_{kt}}. \qquad \text{(B3)}$$

An RPSS of 0 represents no improvement of forecast skill relative to climatology. An RPSS greater than 0 demonstrates improvement of the forecast relative to climatology; an RPSS of 1 is a perfect forecast.

Significance of the RPSS values was assessed using a Monte Carlo procedure. The null hypothesis is that the forecasts have no greater skill than climatology. Such no-skill forecasts were simulated for each forecast period by randomly selecting WTD values 500 times from climatology and then binning these values according to climatology. One thousand such forecasts were made, and a mock RPSS was calculated for each. This distribution of mock RPSS values determined the likelihood that a given RPSS value was due to chance.

REFERENCES

Ambroise, B., J. Freer, and K. Beven, 1996: Application of a generalized TOPMODEL to the small Ringelbach catchment, Bosges, France. *Water Resour. Res.,* **32,** 2147–2159.

Anderson, E., and D. Baker, 1967: Estimating incident terrestrial radiation under all atmospheric conditions. *Water Resour. Res.,* **3,** 975–988.

Barnett, T. P., and R. Preisendorfer, 1987: Origins and levels of monthly and seasonal forecast skill for United States surface air temperatures determined by canonical correlation analysis. *Mon. Wea. Rev.,* **115,** 1825–1850.

Barnston, A. G., M. H. Glantz, and Y. X. He, 1999: Predictive skill of statistical and dynamical climate models in SST forecasts during the 1997/98 El Niño episode and the 1998 La Niña onset. *Bull. Amer. Meteor. Soc.,* **80,** 217–243.

Berri, G. J., and E. A. Flamenco, 1999: Seasonal volume forecast of the Diamante River, Argentina, based on El Niño observations and predictions. *Water Resour. Res.,* **35,** 3803–3810.

Beven, K. J., 1986a: Hillslope runoff processes and flood frequency characteristics. *Hillslope Processes,* A. D. Abrahams, Ed., Allen and Unwin, 187–202.

——, 1986b: Runoff production and flood frequency in catchments of order n: An alternative approach. *Scale Problems in Hydrology,* V. K. Gupta et al., Eds., D. Reidel, 107–131.

——, and M. J. Kirkby, 1979: A physically based, variable contributing area model of basin hydrology. *Hydrol. Sci. J.,* **24,** 43–69.

Chiew, F. H. A., T. C. Piechota, J. A. Dracup, and T. A. McMahon, 1998: El Niño Southern Oscillation and Australian rainfall, streamflow and drought: Links and potential for forecasting. *J. Hydrol.,* **204,** 138–149.

Da Silva, C. C., and E. de Jong, 1986: Comparison of two computer models for predicting soil water in a tropical monsoon climate. *Agric. For. Meteor.,* **36,** 249–262.

Day, G. N., 1985: Extended streamflow forecasting using NWSRFS. *ASCE J. Water Resour. Plann. Manage.,* **111,** 157–170.

DeGaetano, A., K. Eggleston, and W. Knapp, 1995: Daily solar radiation estimates for the northeastern United States using the Northeast Regional Climate Center and National Renewable Energy Laboratory models. *Sol. Energy,* **55,** 185–194.

Ducharne, A., R. D. Koster, M. J. Suarez, M. Stieglitz, and P. Kumar, 2000: A catchment-based approach to modeling land surface processes. Part II: Parameter estimation and model demonstration. *J. Geophys. Res.,* **105,** 24 823–24 838.

Green, P. M., D. M. Legler, C. J. Miranda, and J. J. O'Brien, 1997: The North American climate patterns associated with the El Niño–Southern Oscillation. Project Rep. Series 97-1, Center for Ocean–Atmospheric Prediction Studies, 8 pp.

Hamlet, A. F., and D. P. Lettenmaier, 1999: Columbia River streamflow forecasting based on ENSO and PDO climate signals. *ASCE J. Water Resour. Plann. Manage.,* **125,** 333–341.

Hastenrath, S., 1990: Diagnostics and prediction of anomalous river discharge in northern South America. *J. Climate,* **3,** 1080–1096.

Krzysztofowicz, R., 1983: A Bayesian Markov model of the flood forecast process. *Water Resour. Res.,* **19,** 1455–1465.

——, 1991: Drought forecasting—Methodological topics from a systems perspective. *Stochastic Hydrol. Hydraul.,* **5,** 267–279.

——, and L. M. Watada, 1986: Stochastic model of seasonal runoff forecasts. *Water Resour. Res.,* **22,** 296–302.

Liu, Z. J., J. B. Valdes, and D. Entekhabi, 1998: Merging and error analysis of regional hydrometeorologic anomaly forecasts conditioned on climate precursors. *Water Resour. Res.,* **34,** 1959–1969.

Lynch-Stieglitz, M., 1994: The development and validation of a simple snow model for the GISS GCM. *J. Climate,* **7,** 1842–1855.

Mason, S. J., L. Goddard, N. E. Graham, E. Yulaeva, L. Q. Sun, and P. A. Arkin, 1999: The IRI seasonal climate prediction system and the 1997/98 El Niño event. *Bull. Amer. Meteor. Soc.,* **80,** 1853–1873.

McLean, R. G., and G. S. Bowen, 1980: Vertebrate hosts. *St. Louis Encephalitis,* T. P. Monath, Ed., American Public Health Association, 381–450.

Mitchell, K., and Coauthors, 1999: GCIP Land Data Assimilation System (LDAS) Project now underway. *GEWEX News Bulletin,* Vol. 9, No. 4, 3–6.

Piechota, T. C., F. H. S. Chiew, J. A. Dracup, and T. A. McMahon, 1998: Seasonal steamflow forecasting in eastern Australia and the El Niño–Southern Oscillation. *Water Resour. Res.,* **34,** 3035–3044.

Pitman, A. J., Z.-L. Yang, J. G. Cogley, and A. Henderson-Sellers, 1991: Description of bare essentials of surface transfer for the Bureau of Meteorological Research Centre AGCM. Bureau of Meteorological Research Centre Research Rep. 32, Melbourne, Australia, 132 pp.

Rajagopalan, B., U. Lall, and S. E. Zebiak, 2002: Categorical climate forecasts through regularization and optimal combination of multiple GCM ensembles. *Mon. Wea. Rev.,* **130,** 1792–1811.

Richey, J. E., C. Nobre, and C. Deser, 1989: Amazon River discharge and climate variability—1903 to 1985. *Science,* **246,** 101–103.

Ropelewski, C. F., and M. S. Halpert, 1986: North American precipitation and temperature patterns associated with the El Niño/Southern Oscillation (ENSO). *Mon. Wea. Rev.,* **114,** 2352–2362.

——, and ——, 1989: Precipitation patterns associated with the high index phase of the Southern Oscillation. *J. Climate,* **2,** 268–284.

Schaake, J., and L. Larson, 1998: Ensemble streamflow prediction (ES): Progress and research needs. Preprints, *Special Symp. on Hydrology,* Phoenix, AZ, Amer. Meteor. Soc., J19–J24.

Schmidt, N., E. K. Lipp, J. B. Rose, and M. E. Luther, 2001: ENSO influences on seasonal rainfall and river discharge in Florida. *J. Climate,* **14,** 615–628.

Shaman, J., J. F. Day, and M. Stieglitz, 2002a: Drought-induced amplification of Saint Louis encephalitis virus, Florida. *Emerging Infect. Dis.,* **8,** 575–580.

——, M. Stieglitz, V. Engel, R. Koster, and C. Stark, 2002b: Representation of stormflow and a more responsive water table in a TOPMODEL-based hydrology model. *Water Resour. Res.,* **38,** 1156, doi:10.1029/2001WR000636.

Simpson, H. J., M. A. Cane, A. L. Herczeg, S. E. Zebiak, and J. H. Simpson, 1993: Annual river discharge in southeastern Australia related to El Niño–Southern Oscillation forecasts of sea-surface temperatures. *Water Resour. Res.,* **29,** 3671–3680.

Sivapalan, M., K. Beven, and E. F. Wood, 1987: On hydrologic similarity, 2. A scaled model of storm runoff production. *Water Resour. Res.,* **23,** 2266–2278.

Smith, J. A., G. N. Day, and M. D. Kane, 1992: Nonparametric framework for long-range streamflow forecasting. *ASCE J. Water Resour. Plann. Manage.,* **118,** 82–92.

Stieglitz, M., D. Rind, J. Famiglietti, and C. Rosenzweig, 1997: An efficient approach to modeling the topographic control of surface hydrology for regional and global climate modeling. *J. Climate,* **10,** 118–137.

——, A. Giblin, J. Hobbie, M. Williams, and G. Kling, 2000: Simulating the effects of climate change and climate variability on carbon dynamics in Arctic tundra. *Global Biogeochem. Cycles,* **14,** 1123–1136.

——, A. Ducharne, R. Koster, and M. Suarez, 2001: The impact of detailed snow physics on the simulation of snow cover and subsurface thermodynamics at continental scales. *J. Hydrometeor.,* **2,** 228–242.

Sumner, D. M., 2001: Evapotranspiration from a cypress and pine forest subjected to natural fires, Volusia County, Florida, 1998–99. U.S. Geological Survey, Water Resources Investigations Rep. 01-4245, Tallahassee, FL, 55 pp.

Tarboton, D. G., cited 2001: TARDEM, a suite of programs for the analysis of digital elevation data. [Available online at http://www.engineering.usu.edu/dtarb/tardem.html.]

Wilks, D. S., 1995: *Statistical Methods in the Atmospheric Sciences.* Academic Press, 467 pp.

Young, K. C., and R. L. Gall, 1992: A streamflow forecast model for central Arizona. *J. Appl. Meteor.,* **31,** 465–479.